NeuroImage 89 (2014) 216–225

Contents lists available at ScienceDirect

NeuroImage

journal homepage: www.elsevier.com/locate/ynimg

Optimization of multifocal transcranial current stimulation for weighted cortical pattern targeting from realistic modeling of electric fields

Giulio Ruffini [a,b,*], Michael D. Fox [c,d], Oscar Ripolles [b], Pedro Cavaleiro Miranda [b,e], Alvaro Pascual-Leone [d,f]

[a] Starlab Barcelona, C. Teodor Roviralta 45, 08022 Barcelona, Spain
[b] Neuroelectrics Barcelona, C. Teodor Roviralta 45, 08022 Barcelona, Spain
[c] Massachusetts General Hospital, Brigham and Women's Hospital, Harvard Medical School, Boston, MA, USA
[d] Berenson-Allen Center for Noninvasive Brain Stimulation, Beth Israel Deaconess Medical Center, Harvard Medical School, Boston, MA, USA
[e] Instituto de Biofisica e Engenharia Biomédica, Faculdade de Ciências da Universidade de Lisboa, 1749-016 Lisbon, Portugal
[f] Institut Guttmann, Hospital de Neurorehabilitació, Institut Universitari adscrit a la Universitat Autònoma de Barcelona, Barcelona, Spain

ARTICLE INFO

Article history:
Accepted 3 December 2013
Available online 15 December 2013

Keywords:
tCS
tDCS
tACS
Transcranial direct current stimulation
Transcranial alternating current stimulation
Electric fields
Targeted stimulation
Multifocal stimulation
Human head model
TES
NIBS
fMRI
PET
rs-fcMRI

ABSTRACT

Recently, multifocal transcranial current stimulation (tCS) devices using several relatively small electrodes have been used to achieve more focal stimulation of specific cortical targets. However, it is becoming increasingly recognized that many behavioral manifestations of neurological and psychiatric disease are not solely the result of abnormality in one isolated brain region but represent alterations in brain networks. In this paper we describe a method for optimizing the configuration of multifocal tCS for stimulation of brain networks, represented by spatially extended cortical targets. We show how, based on fMRI, PET, EEG or other data specifying a target map on the cortical surface for excitatory, inhibitory or neutral stimulation and a constraint on the maximal number of electrodes, a solution can be produced with the optimal currents and locations of the electrodes. The method described here relies on a fast calculation of multifocal tCS electric fields (including components normal and tangential to the cortical boundaries) using a five layer finite element model of a realistic head. Based on the hypothesis that the effects of current stimulation are to first order due to the interaction of electric fields with populations of elongated cortical neurons, it is argued that the optimization problem for tCS stimulation can be defined in terms of the component of the electric field normal to the cortical surface. Solutions are found using constrained least squares to optimize current intensities, while electrode number and their locations are selected using a genetic algorithm. For direct current tCS (tDCS) applications, we provide some examples of this technique using an available tCS system providing 8 small Ag/AgCl stimulation electrodes. We demonstrate the approach both for localized and spatially extended targets defined using rs-fcMRI and PET data, with clinical applications in stroke and depression. Finally, we extend these ideas to more general stimulation protocols, such as alternating current tCS (tACS).

Introduction

Transcranial current stimulation (tCS) is a noninvasive brain stimulation technique in which weak, constant or slowly varying electrical currents are applied to the brain through the scalp. tCS includes a family of related non-invasive techniques including direct (tDCS), alternating (tACS) and random noise current stimulation (tRNS). These techniques use scalp electrodes with electrode current intensity to area ratios of about 0.3–5 A/m^2 at low frequencies (typically <1 kHz) resulting in weak electric fields in the brain, with amplitudes of about 0.2–2 V/m (see Miranda et al. (2013) and Ruffini et al. (2013) and references therein). The neuromodulatory effect of these fields has been confirmed in many laboratories (Antal et al., 2008; Nitsche and Paulus, 2001, 2000; Terney et al., 2008). In a typical tDCS experiment, a continuous current of 1–2 mA is applied for up to 20 min through two large stimulation electrodes (25–35 cm^2). For therapeutic applications, such as post-stroke rehabilitation (Khedr et al., 2013) or the treatment of depression (Loo et al., 2012), tDCS is usually applied daily for five days, during one or more weeks.

While tCS interventions typically focus on a single cortical target, it is widely recognized today that many behavioral manifestations of neurological and psychiatric diseases are not solely the result of abnormality in one isolated brain region but represent alterations in brain networks (see, e.g., Fox et al. (2012b) and references therein). In this context, and provided a specification for the location and type of stimulation effects is available, brain networks become the target of neuromodulatory interventions. Advances in neuroimaging technology such as positron emission tomography (PET), electroencephalography (EEG), magneto-encephalography (MEG) and resting-state functional connectivity MRI

* Corresponding author at: Starlab Barcelona, C. Teodor Roviralta 45, 08022 Barcelona, Spain.
E-mail address: giulio.ruffini@starlab.es (G. Ruffini).
URL: http://starlab.es (G. Ruffini).

1053-8119/$ – see front matter © 2013 Elsevier Inc. All rights reserved.
http://dx.doi.org/10.1016/j.neuroimage.2013.12.002

(rs-fcMRI) are allowing us to non-invasively visualize brain networks in humans with unprecedented clarity. In a parallel and timely development, technologies have become available today which enable the use of more than two electrodes for stimulation, making possible multifocal stimulation of brain networks. Determining the ideal configuration of a multi-electrode tCS system, however, is complicated by the fact that transcranial brain stimulation effects are largely non-local due to Ohmic propagation effects. For this reason, optimization algorithms based on precise models and globally defined, cortical targeting data are needed.

As an especially interesting example, we discuss the use of rs-fcMRI seed maps (Fox et al., 2012b; Shafi et al., 2012) for defining cortically extended tCS targets. In contrast to traditional task-based fMRI, resting state fcMRI examines correlations in spontaneous fluctuations in the blood oxygen level dependent (BOLD) signal in the absence of any explicit input or output, while subjects simply rest in the scanner (see, e.g., Buckner et al. (2013), and references therein). A consistent observation is that regions with similar functional properties, such as the left and right motor cortices, exhibit coherent BOLD fluctuations even in the absence of movement under resting conditions. Negative correlations (anti-correlations) between regions with apparent opposing functional properties have also been observed (Fox et al., 2005). Significant rs-fcMRI abnormalities have been identified across almost every major neurological and psychiatric disease (for a review see Fox and Greicius, 2010), and differences across subjects in rs-fcMRI are reproducible across scanning sessions and have been related to individual differences in anatomical connectivity and behavior.

One of the most valuable clinical uses of rs-fcMRI may be to predict how focal brain stimulation will propagate through networks, thus informing the ideal site for stimulation (Fox and Greicius, 2010; Fox et al., 2012b). Recently, Fox et al. (2012b) used rs-fcMRI to identify differences in functional connectivity between effective and less effective DLPFC stimulation sites (M. Fox et al., 2012; Fox et al., 2012b). Significant differences in connectivity were seen with the subgenual cingulate (SG), a region repeatedly implicated in antidepressant response and an effective DBS target (Drevets et al., 2008; Mayberg, 2009; Mayberg et al., 2005). Based on this finding, Fox et al. used rs-fcMRI with the SG to identify theoretically optimal TMS target coordinates in the left DLPFC (Fox et al., 2012a). A similar strategy can be applied to other neurological diseases with effective or potentially effective DBS sites including Parkinson's disease, dystonia, essential tremor, Alzheimer's disease, and even minimally conscious state. An important challenge with this approach is that rs-fcMRI with an effective DBS site does not identify just a single cortical site, but many. In fact, it provides a continuous pattern across the cortical surface of regions that are both positively and negatively correlated with the deep brain stimulation site of interest. Realizing the full potential of this targeting approach thus requires the ability to simultaneously excite or inhibit multiple sites across the surface of the cortex. As we will see below, the same occurs with targets from other imaging techniques, such as PET. While conventional TMS and tDCS technologies allow for only one or two stimulation sites, the multi-electrode approach perfectly complements this scientific and therapeutic need.

The mechanisms underlying the after-effects of tDCS are still the subject of investigation, but in all cases these local changes are brought about by the accumulated action of the applied electric field over time, directly or indirectly. For this reason we focus here on electric field optimization. Moreover, given that there are strong directional effects in the interaction of electric fields and neurons, i.e., neurons are influenced mostly by the component of the electric field parallel to their trajectory (Bikson et al., 2004; Fröhlich and McCormick, 2010; Ranck, 1975; Rattay, 1986; Roth, 1994; Rushton, 1927), and that the effects of tDCS depend on its polarity, knowledge about the orientation of the electric field is crucial in predicting the effects of stimulation. The components of the field perpendicular and parallel to the cortical surface are of special importance, since pyramidal cells are mostly aligned perpendicular to the surface, while many cortical interneurons and axonal projections of pyramidal cells tend to align tangentially (Day et al., 1989; Fox et al., 2004; Kammer et al., 2007). Thus, an important element in modeling is to provide the electric field distribution and orientation relative to the gray matter (GM) and white matter (WM) surfaces (the latter might be important to study the possibility of polarizing corticospinal axons, their collaterals and other projection neurons). In order to do this, we work here with a realistic head model derived from structural MRI images (Miranda et al., 2013) to calculate the tCS electric field components rapidly from arbitrary EEG 10–20 montages. Importantly, this modeling approach allows for fast calculation of electric field components normal and parallel to the GM and WM surfaces.

In what follows, we show how to use neuroimaging data to specify a target map on the cortical surface for excitatory, inhibitory or neutral stimulation, and how, given constraints on the maximal number of electrodes and currents, a solution can be produced with the optimal electrode currents and their locations. The main differences of our approach with other recent efforts stem from a) the overall concept of working with extended, weighted cortical pattern target maps based on fMRI, PET, EEG, MEG or other data, b) the emphasis on optimization of an electric field component as opposed to its magnitude or intensity (as in, e.g., Sadleir et al. (2012)), c) the definition of targets based on a coordinate system relative to the cortical surface, with targets for normal ($E^{\perp}$) and tangential ($E^{\parallel}$) components of electric field (as opposed to "radial or normal to the skull" as in Dmochowski et al. (2011), and d) the use of advanced algorithms to optimize not only currents but also the number and location of electrodes given appropriate constraints. Finally, in the discussion section we address the generalization of these methods to tACS, although in a more exploratory fashion.

Methods

General statement of the problem

The non-invasive stimulation problem can be loosely classified as follows: a) single localized target, b) bipolar or, more generally, multipolar localized targets and c) pattern targeting. An issue that typically arises in the single target case is how to deal with the return current, since the laws of physics require current conservation and thus a minimum of two electrodes need to be applied. The return (or "reference") electrode is normally positioned in an area which is presumed not to play a role (e.g., "over the contralateral supra-orbital region"), and sometimes it is chosen to have a larger area than the "active" one so that its effects diffuse (Nitsche et al., 2007). More modern approaches include the so-called "high-definition tDCS", where a return arrangement of electrodes is placed close to the active electrode (see, e.g., Dmochowski et al. (2011), and references therein) or more general quasi-monopolar montages such as the one described below, which employ an array of optimally-placed return electrodes (see Targeting localized cortical regions section and Fig. 1).

In bipolar or multi-polar targeting, two or more discrete targets are actually sought, some excitatory (anodal) and others inhibitory (cathodal) (as in, e.g., Chib et al. (2013), Ferrucci et al. (2009), Lindenberg et al. (2010) and Mahmoudi et al. (2011)). This situation will normally require the use of small electrodes, as electric field defocusing may be an issue if large electrodes are used. An example is provided below (see Targeting localized cortical regions section and Fig. 2).

More generally, we have the possibility of global cortical targeting designed to achieve a more effective neuromodulatory outcome. In the case of tDCS, such a map may just be a specification of the areas to excite, inhibit, or leave unaffected, with a particular weighting map prioritizing each of them. We provide examples on the use of PET and rs-fcMRI generated target maps in sections Cortical pattern target from PET and Cortical pattern target from rs-fcMRI respectively.

In the following, and without loss of generality, we make the discussion concrete by adopting the *StarStim* device specifications (produced

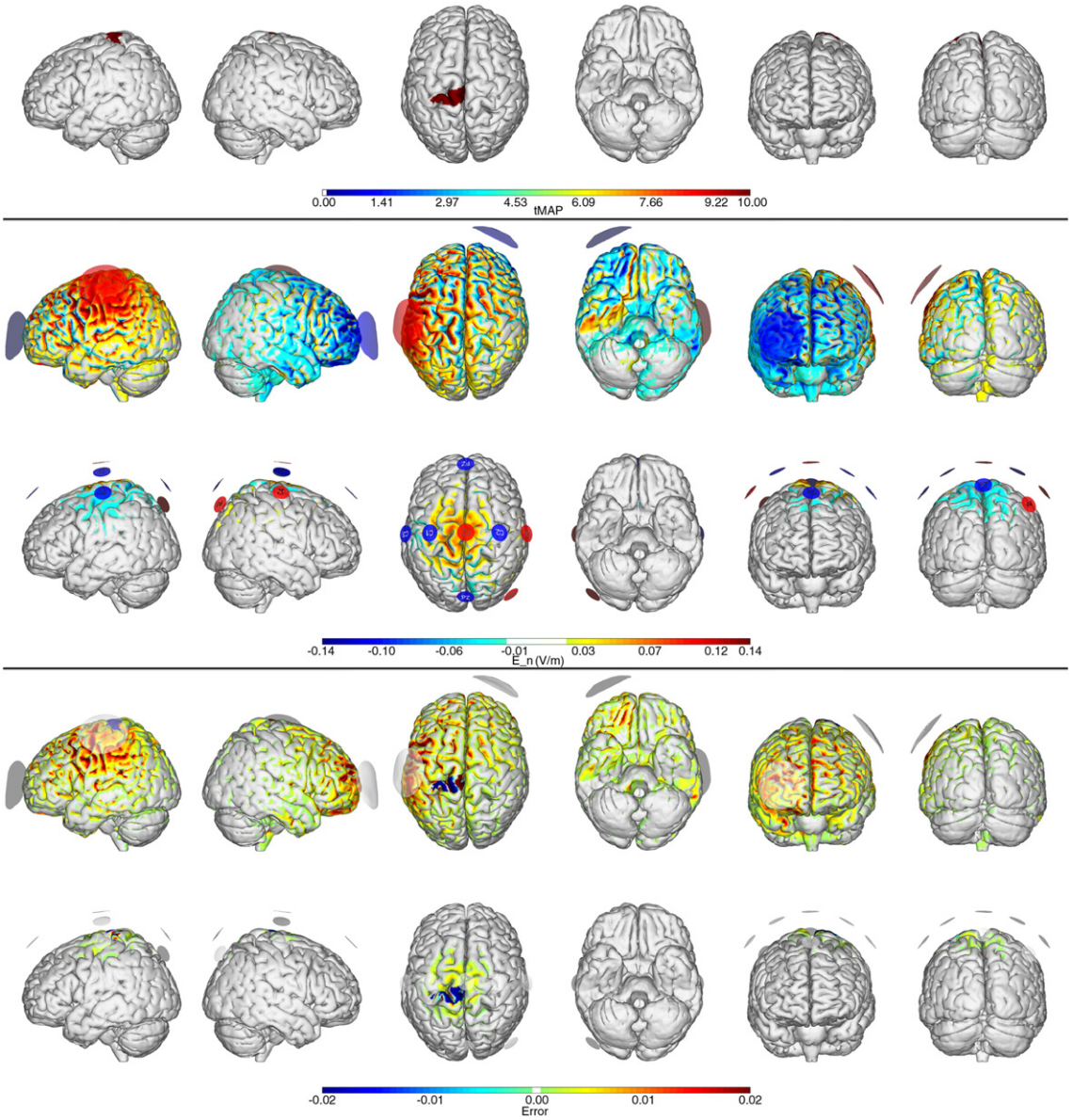

Fig. 1. Montages for unilateral stroke treatment over the left motor cortex. Note the more centralized, "quasi-monopolar" nature of the electric field impact area provided by the 8-electrode solution. First row: target map. Second and third rows: normal electric field maps for a traditional (bipolar) 1 mA montage vs. the 8-electrode optimized solution (1 mA max, 4 mA total max) respectively. Fourth and fifth rows: relative error (ERNI) maps (Err(x) in Eq. (1)) for traditional and 8-electrode solutions respectively. Negative values (blue) indicate a better fit than no intervention, positive values (red) a worse fit than no intervention.

by Neuroelectrics Barcelona, Spain). This device provides up to 8 independently controlled stimulation electrodes (allowing for programmable linear combinations of DC, AC or RNS currents at each electrode). The maximal current delivered by any electrode is 2 mA, while for safety the system constraints the maximal current injected into the brain by all electrodes at any time to 4 mA. The stimulation electrodes (Ag/AgCl "Pi" electrodes, Neuroelectrics Barcelona, Barcelona, Spain) have a radius of 1 cm and provide, through a gel interface, a contact area of π cm^2. The electrodes can be placed on a cap using an extension of the 10–20 system providing 27 default locations.[1]

[1] The list of available positions in the standard *StarStim* cap are (in the EEG 10–10 system): F7, AF7, Fp1, Fpz, Fp2, AF8, F8, F3, Fz, F4, T7, C3, C1, Cz, C2, C4, T8, P7, P3, Pz, P4, P8, PO7, O1, Oz, O2 and PO8.

Realistic head model and electric field modeling

The electric field calculations were performed using the realistic head model described in Miranda et al. (2013). Briefly, tissue boundaries were derived from MR images (scalp, skull, cerebrospinal fluid (CSF) including ventricles, gray matter and white matter) and the Finite Element Method subject to the appropriate boundary conditions was used to calculate the electric potential in the head. Tissues were assumed to be uniform and isotropic and values for their electric conductivity were taken from the literature.

In order to compute electric fields rapidly with our software, we have made use of the principle of superposition. This states that with appropriate boundary conditions, the solution to a general N-electrode problem can be expressed as a linear combination of $N - 1$ bipolar ones. A fixed reference electrode is first chosen, and then all the bipolar solutions using this electrode are computed. A general solution with an arbitrary

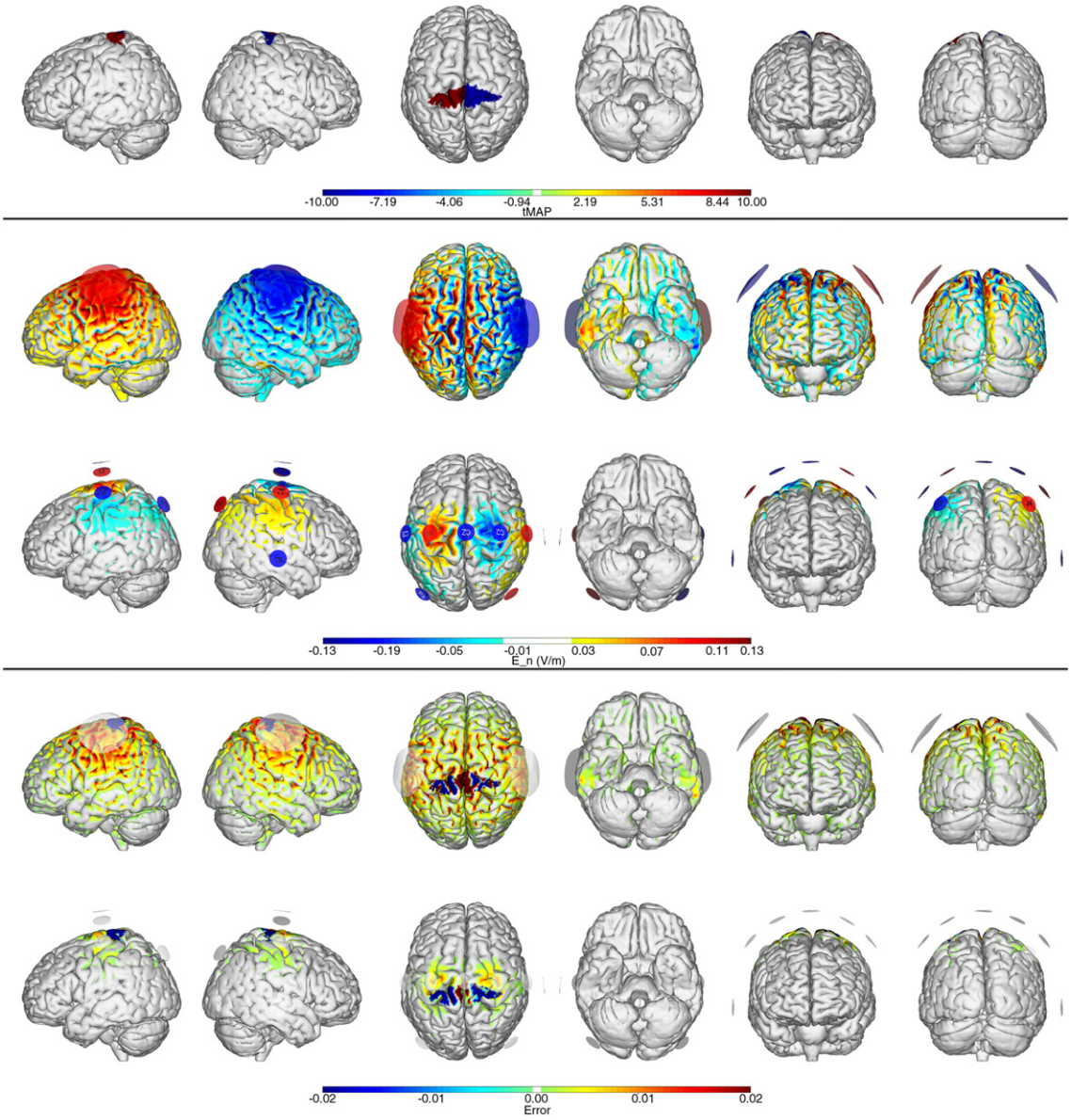

Fig. 2. Montages for bilateral stroke treatment. Note the more centralized nature of the electric field impact area with the multi-electrode solution. First row: target map over the motor cortex on both hemispheres. Second and third rows: normal electric field maps for a traditional (bipolar) 1 mA montage vs. the 8-electrode optimized solution (1 mA max, 4 mA total max) respectively. Fourth and fifth rows: relative error (ERNI) maps (Err(x) in Eq. (1)) for traditional and 8-electrode solutions respectively. Negative values (blue) indicate a better fit than no intervention, positive values (red) a worse fit than no intervention.

number of N electrodes can then easily be computed as follows. The currents to be set can be described by an N-ary array of the form $[I_1,\ldots, I_N]$, with the current conservation constraint $I_N = -\sum_{n=1}^{N-1} I_n$. Let E_n be the electric field solution for a bipolar montage with currents $[0,\ldots +1,\ldots, -1]$ (in some chosen units, with the "+1" in the nth position). For the general multi-electrode case, the electric field due to currents $[I_1,\ldots,I_N]$ is simply given by $E = I_1E_1 + \ldots + I_{N-1}E_{N-1}$.

In our case, 27 "Pi" electrodes were placed on the scalp at the positions available in the standard *StarStim* cap. The electrodes were represented by cylindrical gel disks with a diameter of 1.0 cm and a height of approximately 2.5 mm. Twenty six different calculations were performed, with the anode always at Cz and the cathode at one of the other 26 positions in the cap, and with the current set to 1 mA. The electric field for each one of these bipolar montages was obtained as minus the gradient of the electric potential. The total electric field for a given combination of bipolar montages can then be computed as the weighted vector sum of the electric field due to each montage. A comparison of such superimposed solutions with the direct calculation showed that the errors involved were completely negligible ($<10^{-8}$ V/m). The electric field distributions associated to traditional electrode montages with two 25 cm^2 circular sponge electrodes were also computed in order to compare their performance to the optimized solutions.

In the convention used below, a positive value for the component of the electric field normal to the cortical surface $E^{\perp}$ means that the electric field component normal is pointing *into* the cortex. As we discuss below, such a field would be excitatory. On the other hand, an electric field pointing out of the cortex (negative normal component) would be inhibitory.

Optimization problem and algorithms

The basic mechanism for neuronal interaction in tCS is presently thought to arise from the coupling of electric fields to populations of elongated neurons such as pyramidal cells (Bikson et al., 2004; Molaee-

Ardekani et al., 2013; Radman et al., 2009; Rahman et al., 2013; Roth, 1994; Ruffini et al., 2013 and references therein). Non-coincidentally, such populations are also recognized to be the main generators of EEG signals, in a process of spatially coherent oscillation at certain frequencies (see, e.g., Merlet et al. (2013) and references within). The role of other types of neurons (e.g., interneurons such as basket cells) or other brain cells such as glia is not well understood, since their distribution and connections are complex, but they are in principle less sensitive to such fields due to their more isotropic structures and distributions. Nevertheless, according to this model, a necessary first step in modeling the effects of tCS is to determine the spatial distribution of the generated electric fields in the brain.

At the single neuron level, the external electric field vector forces the displacement of intracellular ions (which mobilize to cancel the intracellular field), altering the neuronal ionic distribution and modifying the transmembrane potential difference. For an ideal straight finite fiber with space constant λ and length $L >> \lambda$ in a locally homogeneous electric field $\vec{E}$, the transmembrane potential difference is largest at the fiber termination, with a value that can be approximated by $\lambda \vec{E} \cdot \hat{n}$, where $\hat{n}$ is the unit vector parallel to the ideal main fiber axis (see Rahman et al. (2013), Ranck (1975), Ruffini et al. (2013) and references therein). This is essentially a first-order Taylor approximation in the electric field, with a spatial scale provided by the membrane space constant λ, and geometric directions by field and fiber orientation. For short neurons of length $L < \lambda$, the spatial scale factor tends to L. Thus, longer neurons with a higher membrane space constant will undergo a larger change in membrane potential.

Ideally, in order to set up a montage optimization problem it would be necessary to fully define the target vectorial electric field values in the cortex (or other areas) based on neurobiophysical principles. With such a specification an optimization problem could easily be defined. However, given our limited understanding of brain function this does not seem possible today. As proxies, desired target values for the magnitude or some of the components of the electric field can be specified. Working with magnitudes is a priori problematic, because the magnitude of the electric field vector or any of its components is invariant under overall current reversal, and there is abundant evidence showing that current direction is an important parameter in tDCS. Indeed, pyramidal neuron populations in the cortical outer layer display a preferred alignment direction normal to the cortical surface. For this reason, they offer a clear target and preferred direction for tCS stimulation. While other electric field components may no doubt be important (Rahman et al., 2013), it does not seem presently possible to determine how to specify these components in any polarity sensitive optimization strategy, given the apparent isotropy of connections in directions other than the normal. For these reasons, and without loss of generality, we choose to focus here on the optimization of the component of the electric field normal to the cortical surfaces.

With the fast electric field calculation algorithm in place, the optimization problem is essentially defined by i) a target map on the cortical surface, ii) a weight map providing the degree of relative importance of each location in the target map and, iii) a set of constraints on the number of electrodes and their currents, as described in Targeting localized cortical regions section.

The target and target weight maps

The target map can be a user-defined area or areas in the cortical surface. Target maps can be defined ad-hoc by the user, or they can stem from, e.g., fMRI, PET, MEG or EEG data, as described in General statement of the problem section. In the latter case techniques such as bandpass filtering and cortical mapping (a simpler version of EEG tomography where the generating dipoles are constrained to the cortical surface) could be used to generate target maps (see the discussion below). Indeed, EEG connectivity analysis can be carried out at the voxel or node level as opposed to electrode space (see, e.g., Ray et al. (2007)).

The use of rs-fcMRI seed *t*-test maps (called here "t-maps") is particularly appealing, as it can provide links to deep regions not easily accessible by non-invasive stimulation techniques. However, seed maps can also be used to target cortical networks. Such applications may be of interest for pathologies such as stroke or epilepsy, with seeds defined by cortical lesions. In this way, stimulation may not only directly target the affected region, but also the entire cortex exploiting brain connectivity.

The algorithm described here requires the provision of a ternary choice. A given area may be stimulated for excitatory, inhibitory or neutral effects. Such choices basically define the targeted electric field normal component at each region. An electric field target value $E_0^{\perp}(x)$ can be defined by the user. Here we will work with a value based on the tCS literature (Miranda et al., 2013), where currents of the order of 1–2 mA are used. For example, $E_0^{\perp} = +0.3$ V/m is a reasonable target for excitation (recall that electric field direction is defined here to be positive if directed normal and inwards at the cortical surface), $E_0^{\perp} = -0.3$ V/m for inhibition, and $E_0^{\perp} = 0$ V/m for a neutral effect. The weights assigned to each location typically vary from 0 to 100, biasing the solutions towards some specific target areas.

Current intensity optimization

Assuming that a set of electrode locations has been specified, we describe here the process of current intensity optimization given target and weight maps. The generic system of equations to solve for a hypothetical N-electrode system is[2] $[E_1(x) \ldots E_{N-1}(x)] \cdot I = E_0(x)$, where $E_n(x)$ is a basis function solution for a particular bipolar combination (specifying the normal component of the E field at each point x in the mesh), I is the array of sought-for currents, and $E_0(x)$ is the target value related to the t-map. We note that in our current implementation there are about 75,000 points in the outer cortical mesh (GM outer surface) and 88,000 in the WM surface (WM–GM interface).

In the case of a statistical t-map $T(x)$ from, e.g., rs-fcMRI, moreover, we request that the equation associated to each mesh point x be weighted by a weight $W(x)$. If the t-map magnitude is large at a given cortical location, we ask that the corresponding equation be enforced strongly, since the location under scrutiny is proportionally statistically significant. This can be implemented by multiplying each row in the target equation above by $W(x) = |T(x)|$. In addition, if the target map at a given location is not statistically significant (e.g., $|T| < 2$) we may want our solution to have no effect on it, that is, the target electric field for a given lower threshold T_{min} should be set to 0. A minimum weight W_{min} should be set for such cases (e.g., $W(x) = W_{min} = 2$).

The problem of optimization of currents for a given montage is formalized using constrained, weighted least squares. Mathematically, the goal is to minimize the Error Relative to No Intervention (ERNI) $\Delta(I) = \sum_x \mathrm{Err}(x;I)$, where we define the local relative error at each mesh point x by (V/m)

$$\mathrm{Err}(x;I) = \frac{(Y_w(x) - E_w(x)I)^2 - (Y_w(x))^2}{(1/N_x)\sum_x W(x)^2.} \quad (1)$$

Here, I is the array of electrode currents, N_x is the number of mesh points and $Y_w(x) = E_0 \mathrm{T}(x)$ if $|\mathrm{T}(x)| > T_{min}$, else $Y_w(x) = 0$, and $E_w(x) = E(x)W(x)$. Optimization is subject to the constraints $|I_n| < I_{max}$ for n = 1,..., N (with $I_N = -\sum_{n=1}^{N-1} I_n$), where I_{max} is the maximal allowed current at any electrode, and $\sum_{I_n>0} I_n = (1/2)\sum_N |I_N| < I_{max}^T$, where I_{max}^T is the maximal allowed total injected current into the brain.

The quantities $\mathrm{Err}(x;I)$ and $\Delta(I)$ as defined provide measures of how close the solution is to the target (at a mesh point or on the average, respectively). Note that the definition is relative to a zero-current solution (no stimulation applied), i.e., $\Delta(I) = 0$ means stimulation is off ($I = 0$,

[2] For simplicity we drop the $\perp$ symbol used to indicate the normal component.

no intervention), $\Delta(I) < 0$ ($\Delta(I) > 0$) means the solution has lower (higher) error than no intervention.

Genetic algorithm

Since in general we will wish to limit the number of electrodes used, a search in the space of electrode locations (montages) needs to be carried out. Genetic algorithms (GAs) are often used to solve such directed search problems and are especially interesting for this problem, since both mutation and cross-over of solutions can be defined meaningfully. In addition, GAs parallelize the search in the rather large space of montages (even for a moderately complex 27 electrode cap the number of different montages with 8 electrodes is very large). Briefly, GAs imitate nature by treating candidate solutions to an optimization problem as individuals endowed with a chromosome which is subject to evolution and natural selection (for an introduction see, e.g., Mitchell (1998)). The genetic algorithm implemented here is based on the definition of a montage by a "DNA" binary string (in this case of dimension $N - 1$) specifying the electrodes to be used. The fitness of a given montage is evaluated by finding the best current values for the chosen electrode locations (as described in the previous section). Cross-over and mutation functions are defined in a natural way to ensure that the offspring of solutions do not violate the constraint of maximal number of electrodes in the solution, yet resemble the parents. Solutions with more than the maximal number of electrodes desired are penalized strongly. The algorithm, implemented in MATLAB (2009) with specifically designed fitness, cross-over and mutation functions, converges rather quickly (in a few hours) and reliably to a solution.

The overall quality of the solution I is quantified by the Error Relative to No Intervention $\Delta(I)$ (recall that $\Delta(I = 0) = 0$). Another goodness-of-fit measure is provided by the related weighted cross correlation coefficient of target map and electric field,

$$cc = \frac{\sum_x Y_w(x) E_w(x) \cdot I}{\sqrt{\sum_x (Y_w(x))^2 \sum_x (E_w(x)) \cdot I)^2}}, \quad (2)$$

a number between −1 and 1. In order to visually assess solution quality as a map over the cortical surface, ERNI maps (i.e., of $\mathrm{Err}(x; I)$) can be used (as seen in the figures).

Results

In this section we provide some solutions using this technique. In Table 1 a summary of the characteristics of each montage is provided, including a "full-cap" 27 channel solution. We can observe that increasing the number of electrodes beyond 8 improves the performance of the solution only marginally for these particular targets, especially the simpler ones (but this may be a reflection of the spatial correlation scales of the target maps). We also note that the differences in weighted cross-correlation coefficient between traditional and multisite montages are quite significant given then large number of mesh points in the calculation (about 75,000), even considering the spatial correlations of target maps or electric fields.

Table 1
Montage comparisons for the four target maps discussed in the text. Weighted Correlation Coefficient (WCC), Error Relative to No Intervention $\Delta(I)$ (V^2/m^2), maximal current at any electrode and total injected current (μA) are provided for traditional (bipolar), 8 and 27 channel solutions.

Target	Montage	WCC	$\Delta(I)$	Max I	Tot Inj I
BA4 left	Traditional	0.02	163	1000	1000
	8 channel	0.31	−8	1000	1297
	27 channel	0.31	−9	1000	2146
BA4 bilateral	Traditional	−0.07	184	1000	1000
	8 channel	0.26	−13	823	1513
	27 channel	0.26	−14	854	2045
rs-fcMRI SG seed map	Traditional	0.11	1	1000	1000
	8 channel	0.29	−214	1000	3262
	27 channel	0.31	−239	1000	4000
PET DBS map	Traditional	−0.05	125	1000	1000
	8 channel	0.21	−51	843	2236
	27 channel	0.23	−59	1000	4000

Targeting localized cortical regions

As discussed, in a typical tDCS study two electrodes are placed on the scalp to target a specific brain region. The effect of the chosen montage depends on the spatial distribution of the vectorial electric field induced in the GM and WM, and since in a bipolar montage the second electrode will carry the same amount of current as the primary electrode, undesired side effects may appear on the "return" or "reference" site. Consider for example targeting the left motor cortex for excitation, a common approach in stroke rehabilitation (Mahmoudi et al., 2011). We choose here the weights in the motor cortex areas to be twice as large as in the rest of the cortex, where the field target is zero. In Fig. 1 we provide a simulation of the electric field using a traditional montage with 25 cm^2 sponges over C3 and FP2 (the contralateral supra-orbital region). We can observe the widespread nature of the induced fields, and the resulting high Error Relative to No Intervention as compared to the GA optimized 8 electrode montage (see Table 1). We note that weighted cross-correlation coefficients remain relatively low even for the best solutions, reflecting the limited freedom available to adapt to the defined weighted target maps. Similarly, Fig. 2 illustrates a bipolar target map used in stroke rehabilitation (e.g., Lindenberg et al. (2010) and Mahmoudi et al. (2011)), with one excitatory target on the left motor cortex, the other (inhibitory) on the right. Again, the multi-electrode solution provides a superior fit, with better account for neutral effect target areas.

Cortical pattern target from PET

We provide in Fig. 3 the solution for a cortical target map based on PET data (Mayberg et al., 2005). The target reflects cerebral blood flow (CBF) changes in response to deep brain stimulation therapy for treatment-resistant major depression. Accordingly, the optimization problem is designed to excite regions where CBF has increased, and inhibit regions where CBF decreases, with target weights proportional to CBF change magnitude. As can be seen in Table 1, the multifocal solution provides a lower Δ and higher correlation coefficient (Table 1) since it is able to "hit" the target map at several locations, while the classical montage performs rather poorly.

Cortical pattern target from rs-fcMRI

Continuing with the example of treatment-resistant major depression, we have generated an electrode montage that will excite and inhibit different areas of the cortex based on the cortical rs-fcMRI t-map pattern of correlation with the SG, with target weights proportional to t-map magnitude. In this case, the rs-fcMRI t-map needs to be sign reversed, since the goal is inhibition of the associated seed. By exciting anti-correlated areas and inhibiting correlated areas, we would hypothesize that this stimulation will propagate to and maximally inhibit the SG, improving antidepressant response. Note that on the basis of this target map there is no obvious rationale for using a traditional montage with anodal stimulation over the left dorsolateral prefrontal cortex (DLPFC)—e.g., the rs-fcMRI target map is fairly symmetric. In Fig. 4 we provide the solution to this problem using an 8 electrode montage as opposed to one using a traditional montage, where we target the left DLPFC as depicted by the left BA46 (F3) with a return over Fp2 (see, e.g., Palm et al. (2012) and Fregni et al. (2006)). Again, the multi-electrode solution yields a lower Δ and higher correlation coefficient than the classical montage (Table 1).

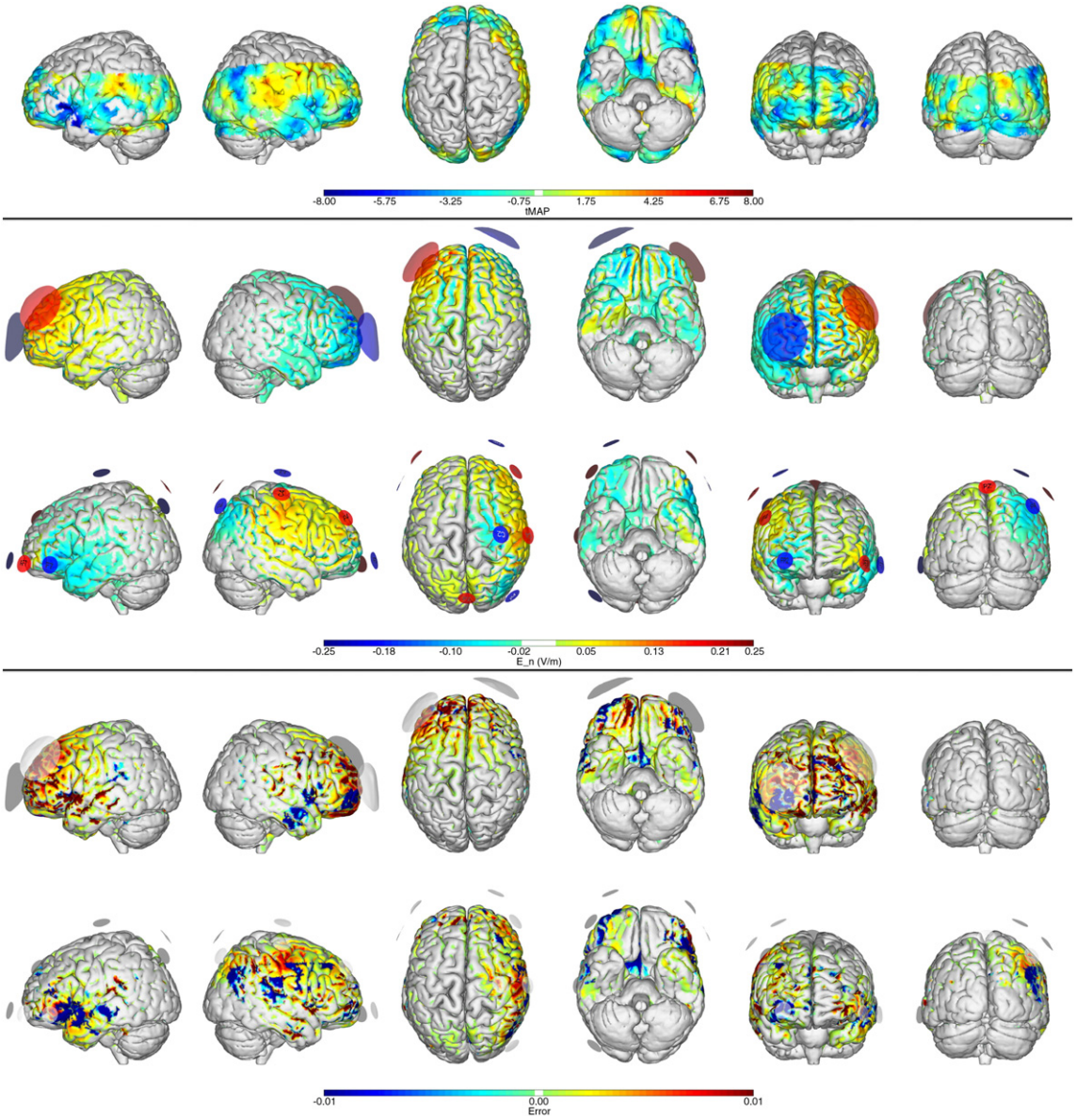

Fig. 3. Montages for depression (from PET data). First row: target map from PET changes in response to DBS therapy for depression. Second and third rows: normal electric field maps for a traditional (bipolar) 1 mA montage vs. the 8-electrode optimized solution (1 mA max, 4 mA total max) respectively. Fourth and fifth rows: relative error (ERNI) maps (Err(x) in Eq. (1)) for traditional and 8-electrode solutions respectively. Negative values (blue) indicate a better fit than no intervention, positive values (red) a worse fit than no intervention.

Discussion

We have described here a method for optimization of tDCS montages with extended targets based on realistic head modeling of the components of the electric field as defined by cortical surfaces. The advantage of working with the electric field on the cortical surface is that it allows for optimization of the normal component of the electric field, or of its tangential component or magnitude. The methodology is based on current knowledge of the primary interaction of tCS electric fields and the cortex. The optimization problem is defined in terms of a target map which attributes weights to the different mesh points. This concept makes the method very flexible and allows for working with one or a few extended uniform targets with simple or arbitrary shapes or, more importantly, with extended targets weighted by some measure of interest such as "activation" or "connectivity" obtained using various imaging modalities, with the ability of specifying the number of electrodes available for stimulation. Focality is achieved by prescribing zero field values at the nodes outside the target for which specific weights can also be specified. Safety in protocol optimization is addressed by limiting the current through each electrode and the total current injected into the brain.

Target maps can be defined from various sources. These include fMRI, EEG—which raises the interesting possibility of closed-loop montage optimization—positron emission tomography (PET) and near-infrared spectroscopy (NIRS) (Shafi et al., 2012). These brain imaging methods can be leveraged to provide information both for clinical or research applications. Magnetic resonance spectroscopy (MRS) can provide another potential means to gather additional, relevant neurochemical information that may help define whether excitatory or inhibitory stimulation should be applied to a given node. Diffusion tensor imaging (DTI) data could be used to refine electric field models to take into consideration conductivity anisotropy and also for defining vectorial (oriented) target maps beyond the cortical normal model. Furthermore, methods for aggregating information from these techniques may provide unique, yet insufficiently explored ways to further refine cortical target maps. Future efforts in this area would be valuable.

Some limitations of the proposed approach should be mentioned here. These include the need for restriction to a set number of fixed

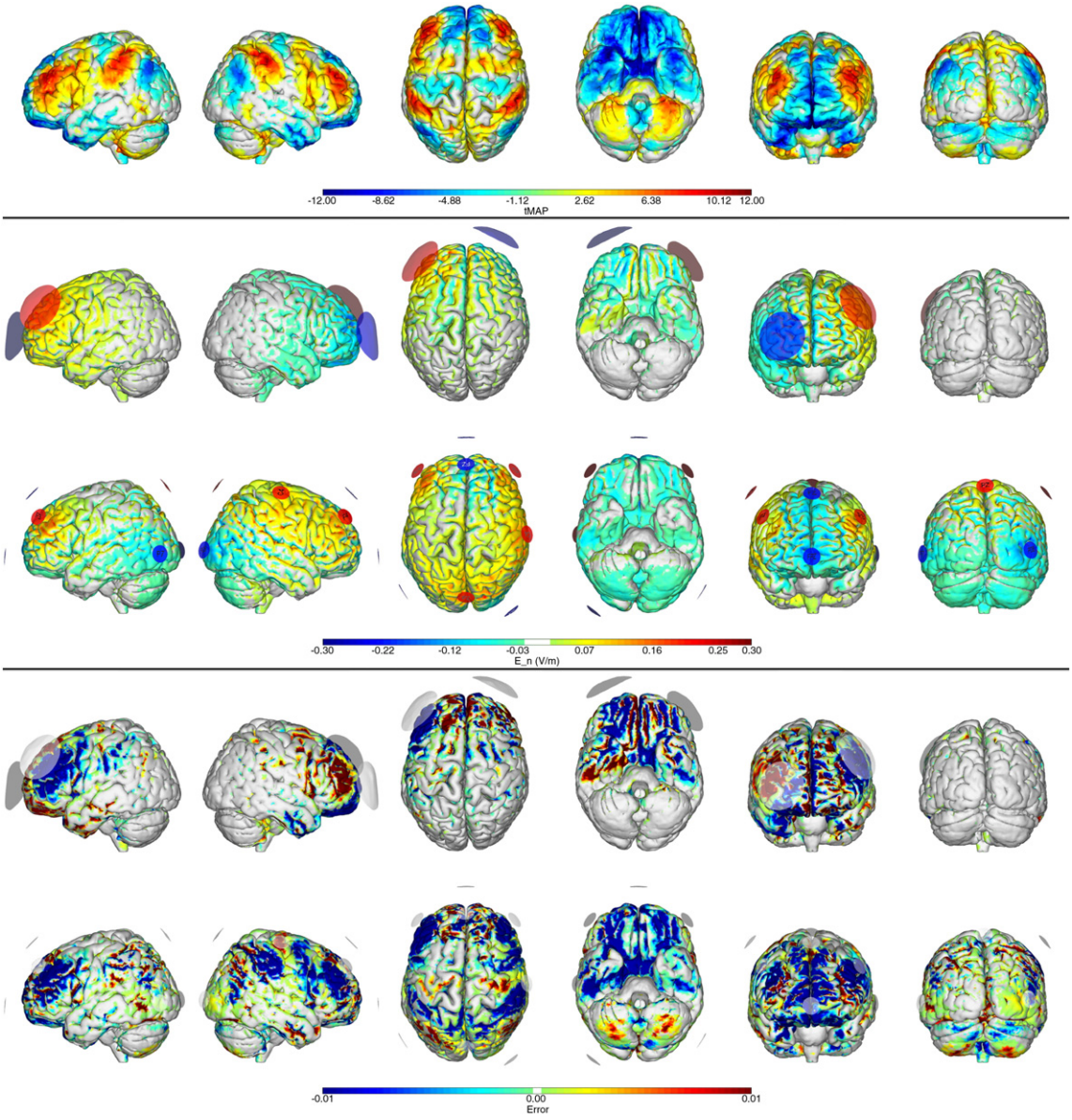

Fig. 4. Montages for depression (from SG rs-fcMRI seed target map). First row: target map. Second and third rows: normal electric field maps for a traditional (bipolar) 1 mA montage vs. the 8-electrode optimized solution (1 mA max, 4 mA total max) respectively. Fourth and fifth rows: relative error (ERNI) maps (Err(x) in Eq. (1)) for traditional and 8-electrode solutions respectively. Negative values (blue) indicate a better fit than no intervention, positive values (red) a worse fit than no intervention.

positions for electrode placement, an optimization based on cortical surface target maps, the focus on normal component of electric fields and the reliance on a specific head model. The first limitation can be overcome by the use of higher density caps, e.g., a 10–10 full cap (74 electrode positions) as opposed to the subset of 27 positions used here. The second limitation is not a critical one given the rather large scale of tCS currents compared to gray matter thickness. However, if deeper structures are sought a volume optimization problem can be defined instead. The focus on the electric field cortical normal component is not a intrinsic limitation of the implementation described here, but rather a choice. The algorithm described here can equally handle optimization of electric field components as well as electric field magnitude. It does remain to be seen which optimization problem is most appropriate, an issue to be elucidated by experimental work.

Even though the realistic simulation of electric fields in the brain is based on solid physics, there is uncertainty on the precise conductivity values to be used. These limitations and others (including the use of isotropic conductivity) in our realistic head modeling are discussed in Miranda et al. (2013). Research is on-going on the sensitivity of electric fields to variability of conductivity variables. There is, nevertheless, a high need to contrast these models with measurements, certainly a topic for further work.

We note that the model used here is based on the single-subject template *Colin27*. Other approaches can be envisioned, such as the use of the MNI-152 average model (Fonov et al., 2009) or, even better, the use of personalized models based on individual scans, which will certainly be necessary in specific cases (e.g., the case of damaged brains or skulls). We also note that in the examples above we have used rs-fcMRI group data to define cortical maps. Target maps may eventually require individualization-e.g., individual differences in rs-fcMRI associated to depression have been reported (M. Fox et al., 2012). However, while individualization in either case may add more precision, it is presently unclear in which cases the extra modeling effort will be warranted, given that tCS fields are rather spatially spread. On the other hand, the normal component of the electric field peaks mainly in the bottom of the sulci, and the main sulci are not too variable among different subjects even though their position in the brain can vary by a few centimeters. Similarly, the fact that targets are generally distributed and large (the

target maps usually display low spatial frequencies) also means that the electric field is in effect "averaged over" the anatomy, making small anatomical details less relevant.

Finally, we note that the basic interaction model used here, where the effects of stimulation are linearly depending on the electric vector field, may not be accurate in all situations. Non-linear effects in electric field or dosage could play a role, e.g., the direction of the excitability change has recently been shown to be intensity dependent (Batsikadze et al., 2013).

Clinical research should explore this methodology in selected interesting applications to test its range of validity, e.g., with pilot tests in depression, Parkinson's disease or stroke. Comparison of effects using traditional versus multifocal montages in healthy subjects would provide an interesting starting point for such research.

Generalization to tACS

The generalization of the proposed method to the case of tACS is non-trivial, even though the process for calculation of electric fields for low frequencies (<1 kHz) is essentially the same as for tDCS. That is, if $E(x)$ is electric field the solution to a DC current for a particular montage and currents, then $E(x,t) = E(x)cos(2\pi tf)$ is the solution to the analogous AC case in which each current is multiplied by $cos(2\pi tf)$. The real difficulty here lies in the choice of a physiological meaningful optimization problem.

Recent studies show that support of brain activity involves the orchestrated oscillatory activity of different and spatially separated brain regions (see, e.g., Buzsaki (2006) and Buzsaki and Draguhn (2004)). Indeed, a major challenge for neuroscience today is to map and analyze the spatio-temporal patterns of activity of the large neuronal populations that are believed to be responsible for information processing in the human brain. Phase or amplitude synchronization may relate different functional regions operating at the same or different frequencies via cross-frequency synchrony. In principle, tACS is potentially capable of acting on such natural rhythms in brain networks through the process of resonance (Antal and Paulus, 2013; Dayan et al., 2013; Fröhlich and McCormick, 2010; Herrmann et al., 2013; Merlet et al., 2013; Paulus, 2011; Ruffini et al., 2013; Zaehle et al., 2010) and devices such as *StarStim* already allow for the simultaneous multisite stimulation of different cortical regions with specific frequencies and relative phases as well as the recording of EEG data from the same electrode locations.

In order to configure properly a multisite monochromatic tACS montage (i.e., one using a single tACS frequency), EEG or MEG data can be used to define the target frequency as well as a target cortical map. The latter could be obtained, e.g., using EEG tomography or cortical mapping algorithms with EEG data filtered at the appropriate frequency band. Closed-loop implementations where the EEG data is used to optimize stimulation parameters can easily be envisioned, with applications such as epilepsy.

In addition, rs-fcMRI data can be used to define a tACS target map much as discussed above. Although fMRI is capable of capturing relatively slow metabolic changes, it has been shown to correlate with local field potentials (LFPs) in the gamma range, and anti-correlate at slow frequencies (Mukamel et al., 2005). It would follow that there are two possible scenarios. For tACS frequencies in the low frequency range (<25 Hz), fMRI and LFP (and presumably EEG) data anti-correlate, hence tACS would be inhibitory with respect to the target map. In the high frequency range (25–300 Hz), tACS would be expected to act in an excitatory fashion. DC stimulation could be combined to target the complementary effect achieved by the chosen tACS frequency. E.g., for high frequency tACS, optimization could be defined by stimulation at the appropriate tACS frequency at the excitatory target map sites, with DC inhibitory stimulation at the complementary sites.

The next order of complexity will involve stimulation at different sites with different frequencies. From the optimization point of view it would suffice to provide target maps for each frequency—the generalization of the least-squares approach described below would be immediate by the principle of superposition (this time in the frequency domain)—with an error function generalized as a weighted sum of error functions for each frequency component.

Going one step further, recent results using resonant "endogenous" stimulation waveforms in vitro (which could be derived from EEG in humans) are particularly intriguing (Fröhlich and McCormick, 2010). While tCS technology allows for all these possibilities, research protocols need to be defined on solid neurophysiological hypotheses, given the large parameter space (which includes the number of electrodes, locations, current intensities and current waveforms).

Acknowledgments

We are very grateful to Helen S. Mayberg for providing the PET data used in this paper. This work was partly supported by the EU FP7 FET Open HIVE project (FET-Open grant 222079) and by the Portuguese Foundation for Science and Technology (FCT). Work on this project was supported in part by Grant Number 8 UL1 TR000170, Harvard Clinical and Translational Science Center, from the National Center for Advancing Translational Science.

Conflict of interest

The content is solely the responsibility of the authors and does not necessarily represent the official views of the National Center for Advancing Translational Science or the National Institutes of Health. GR is co-owner of Starlab and Neuroelectrics and holds patents on multisite tCS. APL serves on the scientific advisory boards for Nexstim, Neuronix, Starlab, and Neosync, and is listed as an inventor on several issued and pending patents on the real-time integration of TMS with EEG and MRI. MDF was supported by grants from the NINDS (R25NS065743, K23NS083741) and the American Brain Foundation. He is listed as an inventor on pending patents on combining TMS and fMRI.

References

Antal, A., Paulus, W., 2013. Transcranial alternating current stimulation (tACS). Front. Hum. Neurosci. 7, 1–4.
Antal, A., Boros, K., Poreisz, C., Chaieb, L., Terney, D., Paulus, W., 2008. Comparatively weak after-effects of transcranial alternating current stimulation (tACS) on cortical excitability in humans. Brain Stimul. 1 (2), 97–105 Apr.
Batsikadze, G., Moliadze, V., Paulus, W., Kuo, M., Nitsche, M., 2013. Partially non-linear stimulation intensity-dependent effects of direct current stimulation on motor cortex excitability in humans. J. Physiol. 591, 1987–2000.
Bikson, M., Inoue, M., Akiyama, H., Deans, J.K., Fox, J.E., Miyakawa, H., Jefferys, J.G., 2004. Effects of uniform extracellular dc electric fields on excitability in rat hippocampal slices in vitro. J. Physiol. 557, 175–190.
Buckner, R.L., Krienen, F.M., Yeo, B.T.T., 2013. Opportunities and limitations of intrinsic functional connectivity MRI. Nat. Neurosci. 16, 832–837.
Buzsaki, G., 2006. Rhythms of the Brain. Oxford University Press Press.
Buzsaki, G., Draguhn, A., 2004. Neuronal oscillations in cortical networks. Science 304, 926–19293.
Chib, V.S., Yun, K., Takahashi, H., Shimojo, S., 2013. Noninvasive remote activation of the ventral midbrain by transcranial direct current stimulation of prefrontal cortex. Transl. Psychiatry 3.
Day, B., Dressler, D., Maertens de Noordhout, A., Marsden, C., Nakashima, K., Rothwell, J., Thompson, P., 1989. Electric and magnetic stimulation of human motor cortex: surface emg and single motor unit responses. J. Physiol. 122, 449–473.
Dayan, E., Censor, N., Buch, E., Sandrini, M., Cohen, L., 2013. Noninvasive brain stimulation: from physiology to network dynamics and back. Nat. Neurosci. 16, 638–644.
Dmochowski, J.P., Datta, A., Bikson, M., Su, Y., Parra, L.C., 2011. Optimized multi-electrode stimulation increases focality and intensity at target. J. Neural Eng. 8.
Drevets, W., Savitz, J., Trimble, M., 2008. The subgenual anterior cingulate cortex in mood disorders. CNS Spectr. 13, 663–681.
Ferrucci, R., Bortolomasi, M., Vergari, M., Tadini, L., Salvoro, B., Giacopuzzi, M., Barbieri, S., Priori, A., 2009. Transcranial direct current stimulation in severe, drug-resistant major depression. J. Affect. Disord. 118, 215–219.
Fonov, V., Evans, A., McKinstry, R., Almli, C., Collins, D., 2009. Unbiased nonlinear average age-appropriate brain templates from birth to adulthood. NeuroImage 47, S102.
Fox, M., Greicius, M., 2010. Clinical applications of resting state functional connectivity. Front. Syst. Neurosci. 4, 19.

Fox, P.T., Narayana, S., Tandon, N., Sandoval, H., Fox, S.P., Kochunov, P., Lancaster, J.L., 2004. Column-based model of electric field excitation of cerebral cortex. Hum. Brain Mapp. 22, 1–14.
Fox, M.D., Snyder, A.Z., Vincent, J.L., Corbetta, M., Essen, D.C.V., Raichle, M.E., 2005. The human brain is intrinsically organized into dynamic, anticorrelated functional networks. Proc. Natl. Acad. Sci. U. S. A. 102, 9673–9678.
Fox, M., Liu, H., Pascual-Leone, A., 2013. Identification of reproducible individualized targets for treatment of depression with TMS based on intrinsic connectivity. NeuroImage 66, 151–160.
Fox, M.D., Buckner, R.L., White, M.P., Greicius, M.D., Pascual-Leone, A., 2012b. Efficacy of transcranial magnetic stimulation targets for depression is related to intrinsic functional connectivity with the subgenual cingulate. Biol. Psychiatry 72.
Fox, M.D., Halko, M.A., Eldaief, M.C., Pascual-Leone, A., 2012c. Measuring and manipulating brain connectivity with resting state functional connectivity magnetic resonance imaging (fcMRI) and transcranial magnetic stimulation (TMS). Neuroimage 62, 2232–2243.
Fregni, F., Boggio, P.S., Nitsche, M.A., Marcolin, M.A., Rigonatti, S.P., Pascual-Leone, A., 2006. Treatment of major depression with transcranial direct current stimulation. Bipolar Disord. 8, 203–204.
Fröhlich, F., McCormick, D.A., 2010. Endogenous electric fields may guide neocortical network activity. Neuron 67, 129–143.
Herrmann, C.S., Rach, S., Neuling, T., Strüber, D., 2013. Transcranial alternating current stimulation: a review of the underlying mechanisms and modulation of cognitive processes. Front. Hum. Neurosci. 7, 1–13.
Kammer, T., Vorwerg, M., Herrnberger, B., 2007. Anisotropy in the visual cortex investigated by neuronavigated transcranial magnetic stimulation. Neuroimage 36, 313–321.
Khedr, E., Shawky, O., El-Hammady, D., Rothwell, J., Darwish, E., Mostafa, O., Tohamy, A., 2013. Effect of anodal versus cathodal transcranial direct current stimulation on stroke rehabilitation: a pilot randomized controlled trial. Neurorehabil. Neural Repair 27, 592–601.
Lindenberg, R., Renga, V., Zhu, L., Nair, D., Schlaug, G., 2010. Bihemispheric brain stimulation facilitates motor recovery in chronic stroke patients. Neurology 75, 2176–2184.
Loo, C.K., Alonzo, A., Martin, D., Mitchell, P., Galvez, V., Sachdev, P., 2012. Transcranial direct current stimulation for depression: 3-week, randomised, sham-controlled trial. Br. J. Psychiatry 200, 52–59.
Mahmoudi, H., Haghighi, A.B., Petramfar, P., Jahanshahi, S., Salehi, Z., Fregni, F., 2011. Transcranial direct current stimulation: electrode montage in stroke. Disabil. Rehabil. 33, 1383–1388.
MATLAB, 2009. Version 7.9.0 (R2009b). The MathWorks Inc., Natick, Massachusetts.
Mayberg, H., 2009. Targeted electrode-based modulation of neural circuits for depression. J. Clin. Invest. 119, 717–725.
Mayberg, H.S., Lozano, A.M., Voon, V., McNeely, H.E., Seminowicz, D., Hamani, C., Schwalb, J.M., Kennedy, S.H., 2005. Deep brain stimulation for treatment-resistant depression. Neuron 45, 651–660.
Merlet, I., Birot, G., Salvador, R., Molaee-Ardekani, B., Mekonnen, A., Soria-Frish, A., Ruffini, G., Miranda, P.F.W., 2013. From oscillatory transcranial current stimulation to scalp eeg changes: a biophysical and physiological modeling study. PLoS One 8.
Miranda, P.C., Mekonnen, A., Salvador, R., Ruffini, G., 2013. The electric field in the cortex during transcranial current stimulation. Neuroimage 70, 45–58.
Mitchell, M., 1998. An Introduction to Genetic Algorithms (Complex Adaptive Systems). The MIT Press.
Molaee-Ardekani, B., Márquez-Ruiz, J., Merlet, I., Leal-Campanario, R., Gruart, A., Sánchez-Campusano, R., Birot, G., Ruffini, G., Delgado-García, J.M., Wendling, F., 2013. Effects of transcranial direct current stimulation (tDCS) on cortical activity: a computational modeling study. Brain Stimul. 6, 25–39.
Mukamel, R., Gelbard, H., Arieli, A., Hasson, U., Fried, I., Malach, R., 2005. Coupling between neuronal firing, field potentials, and fMRI in human auditory cortex. Science 309.
Nitsche, M.A., Paulus, W., 2000. Excitability changes induced in the human motor cortex by weak transcranial direct current stimulation, September 15. J. Physiol. 527, 633–639.
Nitsche, M.A., Paulus, W., 2001. Sustained excitability elevations induced by transcranial DC motor cortex stimulation in humans. Neurology 57 (10), 1899–1901 nov 27.
Nitsche, M.A., et al., 2007. Shaping the effects of transcranial direct current stimulation of the human motor cortex. J. Neurophysiol. 97, 3109–3117.
Palm, U., Schiller, C., Fintescu, Z., Obermeier, M., Keeser, D., Reisinger, E., Pogarell, O., Nitsche, M., Möller, H., Padberg, F., 2012. Transcranial direct current stimulation in treatment resistant depression: a randomized double-blind, placebo-controlled study. Brain Stimul. 5, 242–251.
Paulus, W., 2011. Transcranial electrical stimulation (tES – tDCS; tRNS, tACS) methods. Neurophysiol. Rehabil. 21, 602–617.
Radman, T., Ramos, R.L., Brumberg, J.C., Bikson, M., 2009. Role of cortical cell type and morphology in subthreshold and suprathreshold uniform electric field stimulation in vitro. Brain Stimul. 2, 28.
Rahman, A., Reato, D., Arlotti, M., Gasca, F., Datta, A., Parra, L.C., Bikson, M., 2013. Cellular effects of acute direct current stimulation: somatic and synaptic terminal effects. J. Physiol. 591, 2563–2578.
Ranck, J., 1975. Which elements are excited in electrical stimulation of the mammalian central nervous system: a review. Brain Res. 98, 417–440.
Rattay, F., 1986. Analysis of models for external stimulation of axons. IEEE Trans. Biomed. Eng. 33, 974–977.
Ray, C., Ruffini, G., Marco-Pallarés, J., Fuentemilla, L., Grau, C., 2007. Complex networks in brain electrical activity. Europhys. Lett. 79.
Roth, B.J., 1994. Mechanisms for electrical stimulation of excitable tissue. Crit. Rev. Biomed. Eng. 22, 253–305.
Ruffini, G., Wendling, F., Merlet, I., Molaee-Ardekani, B., Mekkonen, A., Salvador, R., Soria-Frisch, A., Grau, C., Dunne, S., Miranda, P., 2013. Transcranial current brain stimulation (tCS): models and technologies. IEEE Trans. Neural. Syst. Rehabil. Eng. 21, 333–345.
Rushton, W.A.H., 1927. The effect upon the threshold for nervous excitation of the length of nerve exposed, and the angle between current and nerve. J. Physiol. 63, 357–377.
Sadleir, R.J., Vannorsdall, T.D., Schretlen, D.J., Gordon, B., 2012. Target optimization in transcranial direct current stimulation. Front. Psychiatry 3.
Shafi, M.M., Westover, M.B., Fox, M.D., Pascual-Leone, A., 2012. Exploration and modulation of brain network interactions with noninvasive brain stimulation in combination with neuroimaging. Eur. J. Neurosci. 35, 805–825.
Terney, T., Chaieb, L., Moliadze, V., Antal, A., Paulus, W., 2008. Increasing Human Brain Excitability by Transcranial High- Frequency Random Noise Stimulation. J. Neurosci. 28 (52), 14147–14155 December 24.
Zaehle, T., Rach, S., Herrmann, C.S., 2010. Transcranial alternating current stimulation enhances individual alpha activity in human eeg. PLos One 5, 1–7.